Structural Characterization and Topology of the Second Potential Membrane Anchor Region in the Thromboxane A_2 Synthase Amino-Terminal Domain

Ke-He Ruan,*,‡ Dawei Li,§ Jie Ji,§ Yue-Zhen Lin,‡ and Xiaolian Gao§

Vascular Biology Research Center and Division of Hematology, Department of Internal Medicine, The University of Texas Health Science Center, Houston, Texas 77030, and Department of Chemistry, University of Houston, Houston, Texas 77204-5641

Received July 31, 1997; Revised Manuscript Received October 13, 1997

ABSTRACT: Thromboxane A_2 synthase (TXAS) has been proposed to have two membrane-bound regions located in the NH_2-terminal domain [Ruan, K.-H., Wang, L.-H., Wu, K. K., and Kulmacz, R. J. (1993) *J. Biol. Chem. 268*, 19483−19489; Ruan, K.-H., Li, P., Kulmacz, J. R., and Wu, K. K. (1994) *J. Biol. Chem. 269*, 20938−20942]. To test this hypothesis, a solution structure in membrane mimetic environments of a synthetic peptide corresponding to the second region of the NH_2-terminal domain (TXAS residues 33−60) has been investigated by circular dichroism (CD), 2D nuclear magnetic resonance (NMR) spectroscopy, and peptidoliposome reconstitution. CD spectroscopy indicated that the peptide adopted a structure with significant α-helical content in 30% trifluoroethanol (TFE) or in dodecylphosphocholine (DPC) micelles, which mimic hydrophobic membrane environment. Through a combination of 2D NMR experiments in the presence of TFE or DPC micelles, complete ^{1}H NMR assignments of the peptide have been obtained and the structure of the peptide has been determined. NH_2-terminal segment of the peptide takes on a well-defined α-helical conformation; the center segment of the peptide, containing three prolines, adopts a bent conformation, and the C-terminal segment of the peptide exists in a mixture of rapidly interconverting conformations. These results provide direct structural evidence that residues 33−60 of the TXAS NH_2-terminal domain contain a second membrane anchor region, with at least residues 35−46 having their helical structure expected for hydrophobic interaction with the membrane. The orientation of the peptide in DPC micelles was evaluated from the effect of incorporation of a spin-label 12-doxylstearate into the micelles. The peptide portions, found to be immersed in the micelles, include the helical segment, the bent segment, and some hydrophobic residues within the C-terminal segment. Two additional synthetic peptides, one corresponding to the NH_2-terminal helical segment (TXAS residues 33−46) and the other including the bent and the C-terminal segments (TXAS residues 47−60) were analyzed for their ability to incorporate into peptidoliposomes. The helical peptide readily incorporated into liposomes; the other peptide did not. These results support the presence of a second functional membrane anchor region localized to the helical segment within TXAS residues 33−46, with passive membrane contacts in the bent and the C-terminal segments of the peptide (TXAS residues 47−60) due to immersion of the helical in the membrane.

TXAS,[1] an endoplasmic reticulum membrane protein, catalyzes the isomerization of prostaglandin H_2 to thromboxane A_2 (TXA_2), a proaggregatory and vasoconstrictive agent. TXA_2 plays an important role in a wide variety of physiological and pathological processes including hemostasis, atherogenesis, thrombosis, and stroke. Elucidation of the structure/function relationship of TXAS is a key step in understanding the pathological processes and developing strategies to control them. TXAS cDNA cloned from human lungs and platelets encodes a 534 amino acid protein with a molecular weight of 60 684 (*3*−*6*). TXAS is a member of the cytochrome P450 superfamily (*7*), with a conserved heme pocket and helical backbone segments (*5*), but it lacks of monooxygenase activity and does not require reductase to initiate the reaction (*7*).

Mammalian P450s are believed to have a large cytoplasmic domain which is anchored to the endoplasmic reticulum

† This work was supported by American Heart Texas Affilitate Inc. Grant 93G-272 and 95R-272 (for K.R.), NIH grant HL56712 (for K.R.), and Welch Foundation (for X.G.). The NMR facility at University of Houston is founded by the W. M. Keck Foundation.

* To whom correspondence should be addressed: Division of Hematology, Department of Internal Medicine, The University of Texas Health Science Center at Houston, 6431 Fannin St., Houston, TX 77030. Tel: 713-792-5450. Fax: 713-500-6810. E-mail: kruan@imed2010.med.uth.tmc.edu.

‡ The University of Texas Health Science Center.

§ University of Houston.

[1] Abbreviations: CD, circular dichroism; COSY, correlated spectroscopy; DPC, dodecylphosphocholine; DQF-COSY, double-quantum filtered COSY; ER, endoplasmic reticulum; HPLC, high pressure liquid chromatography; NMR, nuclear magnetic resonance; NOE, nuclear overhauser effect; NOESY, nuclear overhauser effect correlation spectroscopy; PC, phosphatidylcholine; PE, phosphatidylethanolamine; PS, phosphatidylserine; TFA, trifluoroacetic acid; TOCSY, total correlation spectroscopy; TXAS, thromboxane A_2 synthase; 2D, two dimensional.

S0006-2960(97)01881-3 CCC: $15.00
Published on Web 01/06/1998

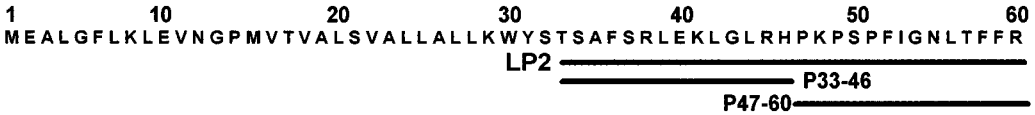

FIGURE 1: Amino acid sequence of the TXAS NH_2-terminal region. The underlines indicate the length of the *LP2* peptide (residues 33−60) and the two short peptides, *P33*−46 (residues 33−46) and *P47*−60 (residues 47−60), used to mimic different portions of the NH_2-terminal region.

membrane by either one or two NH_2-terminal hydrophobic segment(s) (*8*). The first putative anchor region of TXAS and other membrane-bound P450s (about 30 residues from NH_2-terminus) contains many hydrophobic residues, and it is generally accepted that this region indeed comprises a membrane anchor segment. However, there is also a second potential membrane anchor region around residues 33−60 in the NH_2-terminal domain of membrane-bound P450s. Much of current controversy regarding the P450 NH_2-terminal anchor centers on whether the second NH_2-terminal domain region actually functions as a membrane anchor.

In the case of TXAS, antibodies directed against the first 10 and 15 amino acid residues at the NH_2-terminus recognized their epitopes on the cytoplasmic site of endoplasmic reticulum (*1*). In addition, peptides corresponding to both the first (residues 1−36) and the second (residues 33−60, LP2) putative NH_2-terminal membrane anchor regions (Figure 1) adopted significant helical structure in a hydrophobic environment and bound tightly to lipid vesicles by using circular dichroism (CD) spectroscopy and peptido-liposome reconstitution (*2*). These results supported a membrane anchor model for TXAS which has two anchor regions in the NH_2-terminal domain.

One prototypical structure for a membrane anchor element is a helix whose hydrophobic side chains interact with the hydrocarbon interior of a phospholipid bilayer. To provide direct evidences for such a structure in the second putative anchor region of TXAS, CD, and 2D NMR spectroscopy were used to determine the solution structure of a synthetic peptide corresponding to the TXAS segment in a membrane-mimetic environments. The results suggest that the putative second membrane anchor region of TXAS is most likely to contain an α-helical segment which is capable of functional interaction with a lipid bilayer.

MATERIALS AND METHODS

Materials. DPC was purchased from Avanti Polar Lipids (Alabaster, AL); DPC-d_{38}, trifluoroethanol-d_3 (TFE-d_3) and D_2O were from Cambridge Isotope Laboratories (Andover, MA); 12-doxylstearic acid and trifluoroethanol (TFE) were obtained from Sigma (St. Louis, MO). Trifluoroacetic acid (TFA) was obtained from Millipore (Bedford, MA).

Peptide Synthesis. Peptides were synthesized manually using fluorenylmethoxycarbonyl-polyamide solid phase methods (*9*−*11*). After cleavage with TFA, the peptides were purified to homogeneity by HPLC on a Vydac C4 reversed phase column with a gradient of 0 to 80% acetonitrile in 0.1% TFA. Molecular weights of the purified peptides were determined by fast atom bombardment mass spectrometry (*12*). The sequences of the synthesized TXAS LP2 peptide is shown in Figure 1.

Circular Dichroism. Circular dichroism (CD) spectra were recorded on a JASCO-700C spectrometer at ambient temperature in a 0.1 cm path length cell (*13*) and analyzed according to the method developed by Chen et al. (*14*).

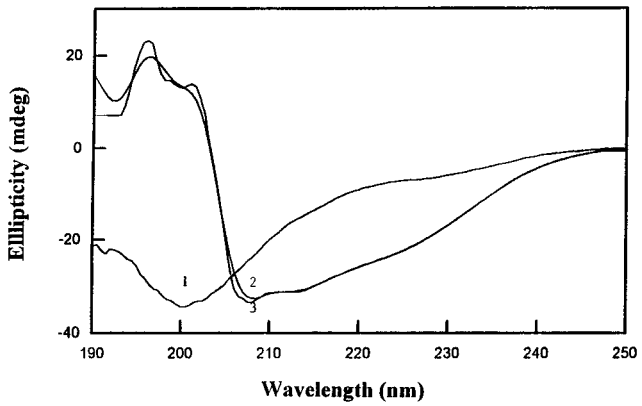

FIGURE 2: CD spectra of TXAS LP2 peptide. Peptide LP2 (100 μM) was dissolved in 0.02 M potassium phosphate buffer, pH 5.5 (spectrum 1), containing 30% TFE (spectrum 2) or 150 mM DPC micelles (spectrum 3). The method was described in the text.

NMR Sample Preparation. The HPLC-purified peptide was dissolved in water and lyophilized three times to completely remove TFA and acetonitrile and then dissolved in 0.02 M sodium phosphate buffer, pH 5.5. The sample was lyophilized and rehydrated at a final concentration of 5 mM in H_2O containing 10% D_2O and 30% TFE-d_3 or 550 mM DPC-d_{38}. For D_2O experiment, the peptide was dissolved in buffer, lyophilized, and then dissolved with 30% TFE-d_3 in D_2O.

NMR Experiments. Proton NMR experiments were carried out on a Bruker AMX-600 spectrometer. All 2D experiments (DQF-COSY, TOCSY, and NOESY) were performed under identical conditions (temperature 289 K and pH 5.5) in H_2O or D_2O solvents. NOESY spectra were recorded with mixing time of 150 and 250 ms. TOCSY spectra were carried out with MLEV-16 mixing sequence with total mixing time of 80 ms. All spectra were composed of 2048 complex points in the F2 dimension and 512 real points in the F1 dimension with 32−128 scans per t1 increment. Quadrature detection was achieved in F1 by the TPPI method. The NMR data were processed using Felix95 (Molecular Simulation, Inc., San Diego, CA). All FIDs were zero-filled to $2k \times 2k$ before Fourier transformation and 0−30° (for DQF-COSY and TOCSY) or 90° (for NOESY) shifted sine-bell window function was used in both dimensions. The sequence-specific assignment was obtained using standard methods (*15*).

Interaction of the LP2 peptide with the interior of DPC micelles was analyzed from the effects of the hydrophobic spin-label probe, 12-doxylstearic acid, on the 2D ^1H NMR of the peptide using the approach described by Chupin *et al.* (*16*, *17*). Briefly, after recording of NOESY (mixing time 250 ms) and TOCSY (80 ms mixing time) spectra of the LP2 peptide in DPC micelles in the absence of the spin label, 0.003 mL of the 12-doxylstearic acid in methanol-d_4 was

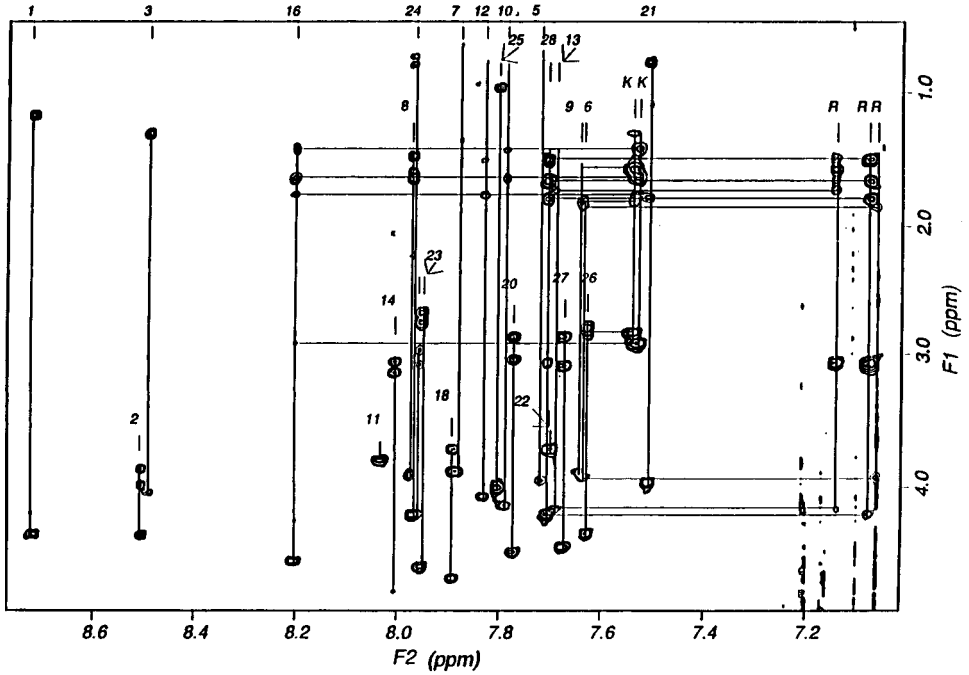

FIGURE 3: Contour plot of a 600 MHz TOCSY spectrum for 4 mM TXAS LP2 in TFE/H_2O at 289 K. The spectral region (F1 = 0.5−4.9 ppm, F2 = 7.0−8.8 ppm) contains cross-peaks connecting intraresidue α-protons and aliphatic side chain protons with amide proton. Each vertical line has been labeled in the spectrum corresponding to the residue numbers in LP2. The capital letters K and R indicate the correlation of side chain amino protons of Lys and Arg with the α-aliphatic side chain protons.

added into the NMR sample (0.5 mL), and another set of NOESY and TOCSY spectra was recorded. The 1:80 molar ratio of DPC detergent to 12-doxylstearic acid provided an average of about 1 molecule of spin-label reagent per DPC micelle. The samples were kept in an N_2 atmosphere to avoid oxidation of the spin label.

Calculation of Structures. The overall structure of the peptide was determined through the use of the intraresidue and sequential NOEs. The Felix 95 program was used for quantification of the NOE cross-peak volumes and for converting them into upper bounds of the interproton distances. NOE cross-peaks were segmented using a statistical segmentation function and characterized as strong, medium, and weak, corresponding to upper bound distance range constraints of 2.7, 3.5, and 5.0 Å, respectively. Lower bounds between nonbonded atoms were set to their van der Waals radii (approximately 1.8 Å). Pseudoatom corrections were added to interproton distance restraints where necessary (*18*). Distance geometry calculations were carried out on an SGI workstation using DGII and NMR refinement programs within Insight II package (Molecular Simulation, Inc., San Diego, CA). A total of 210 NOE constraints and torsion angle restraints derived from couping constants was used for the initial structures calculated from the DGII program. Energy refinement calculations including restrained minimization/dynamics were carried out in the best distance geometry structures using Discover 3 programs within the Insight II package.

Preparation and Characterization of Peptidoliposomes. Peptidoliposomes were prepared as previously described (*2*). In brief, phosphatidylcholine, phosphatidylethanolamine, and phosphatidylserine were dissolved in a small volume of chloroform/methanol (1:1), and the solvent was then evaporated with a steam of nitrogen gas. An appropriate amount of peptide dissolved in 1.6 mL of 0.1 M sodium phosphate buffer, pH 7.4, containing 20% glycerol and 20% sodium cholate, was added to the dried lipid to give a lipid:peptide ratio of 5:1(w/w). After incubation overnight, the mixture was dialyzed against 20 mM Hepes, pH 8.0, containing 0.1 mM EDTA and purified by gel filtration on a Sepharose 6B column. Eluting peptide was monitored from the absorbance at 220 nm, and eluting lipid was monitored from the fluorescence after addition of diphenylhexatriene (*2*, *19*).

RESULTS

CD Spectroscopy Analysis. CD spectroscopy studies indicate that the presence of TFE induces helical secondary structure in a significant portion of LP2 peptide (Figure 2) (*2*). The CD spectrum of LP2 peptide in DPC is clearly rather similar to that obtained in TFE. The helical content of LP2 in DPC was estimated to be about 30%. It is thus apparent that the helical structure induced in the peptide LP2 by TFE, which mimics the homogeneous hydrophobic part of the membrane, is comparable to that induced by DPC micelles, which mimic a heterogeneous amphophilic membrane environment. This validates the uses of TFE and DPC micelles for NMR studies of the LP2 peptide.

NMR Assignment. 2D NMR spectra of the peptide was recorded in the presence of TFE-d_3 or DPC-d_{38}. 1H NMR assignments were accomplished for the TFE-d_3 system using the standard sequential assignment technique (*15*, *20*−*22*). The assignment of ^1H in the presence of DPC-d_{38} was made by comparison with the assignments of proton resonances of the peptide in TFE-d_3. This procedure involves identification of spin systems and sequential assignment using a combination of TOCSY (*23*, *24*), DQF-COSY (data not shown) (*25*), and NOESY (*26*) spectra recorded in both H_2O (Figures 3 and 4) and D_2O (data not shown). The complete proton resonance assignments for the peptide in TFE and DPC were summarized in Table 1. An autoassignment

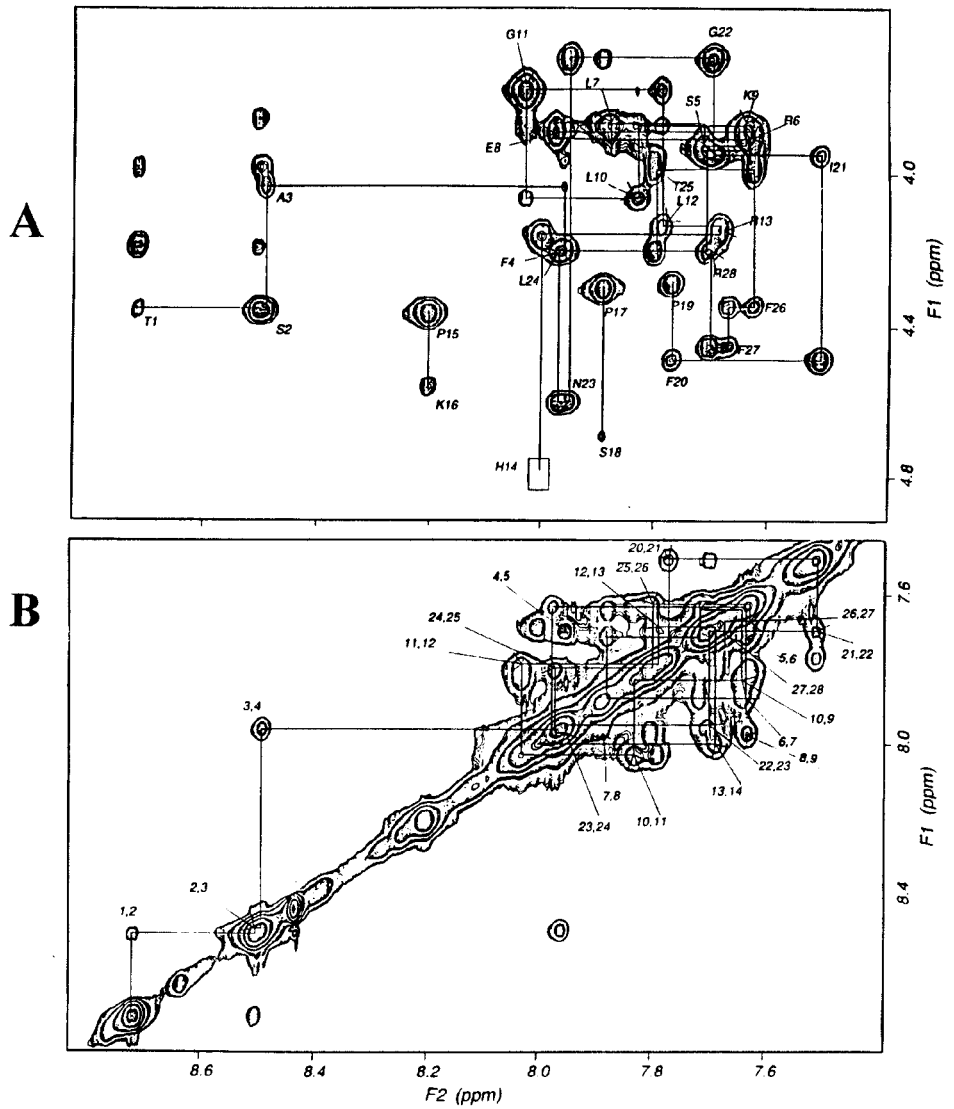

FIGURE 4: (A) Expanded αH-NH region of the NOESY spectrum (150 ms mixing time) for TXAS LP2 in TFE/H_2O. The spectrum was recorded at 289 K. The dαN sequential connectivities are shown. (B) Expanded NH-NH region of the same NOESY spectrum as in panels A, displaying the dNN sequential connectivities.

followed the instructions of the assignment program in the Felix95 package was also used to confirm the above assignments.

Secondary Structure Analysis. Evaluation of secondary structure was carried out in the following steps: (1) identification of interresidue NOE cross-peaks, particularly the αH-NH and αH-βH through space connectivities. A helical structure is characterized by dαN(i,i+2), dαN(i,i+3), dαβ(i,i+3), and dαN(i,i+4) connectivities (*20*, *21*, *27*); (2) qualitative comparison of $^3J_{NH\alpha}$ coupling constants from the NH-αH cross-peaks in the DQF-COSY spectrum. The $^3J_{NH\alpha}$ coupling constants were obtained by direct measurement of $^3J_{NH\alpha}$ values and by comparing the intensities of NH-αH cross-peaks, which are grouped as strong (J > 6 Hz), medium (J = 4−6 Hz), and weak (J < 4 Hz). Weak and strong $^3J_{NH\alpha}$ coupling constants have been used to identify helical and β-sheet structures, respectively (*28*, *29*). It has been well established that chemical shifts, which deviate from "random coil" reference values (conformational shifts), are closely correlated to the type of secondary structure in proteins and peptides (*15*, *27*). In particular, αH and NH conformational shifts have been proposed as markers for characterization of peptide helical structures in solution. Large conformational shift (greater than 0.3 ppm upfield) is a sensitive and powerful sign for the presence of helical structure.

From the data shown in Figure 5, it is apparent that the Hα(i)-Hβ(i+3) NOESY connectivities were similar in TFE and DPC micelles. This indicates that the peptide has comparable secondary structures in the TFE and DPC environments. The medium-range NOE connectivities in NOESY spectra and the strength of the $^3J_{NH\alpha}$ coupling from the NH-CαH cross peaks in the DQF-COSY spectra are summarized in Figure 6A for the peptide in TFE and in Figure 6B for the peptide in DPC micelles. These data suggest that in both the TFE and DPC environments, an α-helical segment (segment I) starts at Ala3 and extends to His14.

There are three proline residues (Pro15, 17, and 19) in segment II (residues 15−20). The conformation of this part of peptide will depend on the conformation of the prolines. Proline can adopt one of the two major conformation, *cis* or *trans*, or adopt the mixture of two due to an *cis-trans* isomerization. The activation energy barrier for isomeriza-

Table 1: Proton Chemical Shifts for LP2 peptide in TFE and DPC Micelles

	TFE					DPC	
residues	HN	Hα	Hβ_1	Hβ_2	others	HN	Hα
Thr1	8.73	4.36	4.20	1.18		8.63	4.41
Ser2	8.51	4.36	3.98	3.86		8.38	4.42
Ala3	8.49	4.04	1.31			8.28	4.02
Phe4	7.97	4.20	2.96			8.28	4.21
Ser5	7.72	3.95			4.20	8.06	4.10
Arg6	7.64	3.92	2.08	1.81	1.48, 0.92	7.62	3.95
Leu7	7.88	3.88	1.48		1.36, 0.66, 0.66	7.69	3.94
Glu8	7.97	4.21	1.47		1.63	8.03	3.98
Lys9	7.64	3.88	1.81		1.49	7.62	3.95
Leu10	7.83	4.07	1.77	1.50	0.76	7.83	4.14
Gly11	8.03	3.78				8.08	3.81
Leu12	7.79	4.14	1.64		1.44, 0.78	7.86	4.23
Arg13	7.69	4.15	1.72	1.60	3.71	7.62	4.00
His14	8.00	4.79	3.14	3.05		7.97	4.34
Pro15		4.42	2.21		1.90	8.47	4.42
Lys16	8.21	4.56	2.92	1.77	1.63, 1.42	8.47	4.24
Pro17		4.42	2.20		1.83	8.41	4.41
Ser18	7.89	4.69	3.87	3.71		8.40	4.24
Pro19		4.37	2.17		1.68	8.34	4.36
Phe20	7.77	4.49	3.04	2.86		8.34	4.44
Ile21	7.51	3.96	1.78		1.10, 0.78	7.92	3.98
Gly22	7.70	4.20			3.70	7.68	4.00
Asn23	7.96	4.60	2.74	2.68		7.92	4.23
Leu24	7.97	4.21	1.64	1.58	1.47, 0.81, 0.71	8.06	4.29
Thr25	7.80	3.99	3.95		0.97	7.78	4.10
Phe26	7.63	4.35	2.84	2.79		7.61	4.51
Phe27	7.67	4.45	3.08	2.85		7.78	4.35
Arg28	7.72	4.21	3.06		1.79, 1.66, 1.4	7.61	4.10

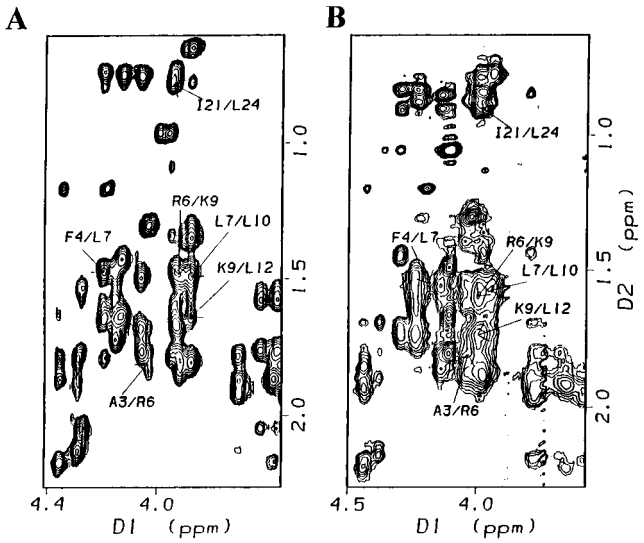

FIGURE 5: Hα-Hβ region of the NOSEY spectra of TXAS LP2 peptide in TFE (A) or DPC micelles (B). Interresidual medium-range Hα(i)-Hβ(i+3) NOEs are indicated.

tion of Xxx-Pro peptide bonds in polypeptides and proteins is in the range 15−20 kcal/mol, and to observe the exchange on the NMR time scale frequently requires elevated temperature. We did not attempt to measure this chemical exchange. Fortunately, we have enough NOE connectivities to determine the conformation of these prolines. Table 2 listed the NOE connectivities for Xxx-Pro pairs. It is clear that all three prolines in LP2 peptide are in *trans* conformation that characterized by relatively short distance (strong NOE) between NH or CαH of Xxx and CδH$_2$(i+1) of Pro (Figure 7A) (*15*). The NOE connections of CαH of Xxxx and CδH$_2$(i+1) of Pro (Figure 7A) indicate that the distance between these protons are short, which reveal that a torsion angle ψi is in the range 180 ± 30° (*15*). We have also observed several NOE connections for CβHi-NHi+1 of Pro-Xaa residue pairs (P15-K16, P17-S18, and P19-F20) (Figure 7B). The medium intensities of CβHi-NHi+1 cross-peak indicate that the torsion angle ψi is in the range of 180 ± 30° (distance 2.2−3.0 A). From Figure 4 we have seen a very strong NOE connection of CαHi-NHi+1 for Pro-Xaa pairs (P15-K16, P17-S18, and P19-F20), which indicate that the torsion angle shall be in the range of 180 ± 30°. The structure of segment II was constructed by taking the facts discussed above. It forms a bend conformation to connect segment I and III.

The observed chemical shifts for the LP2 peptide in TFE or DPC were compared with those for a random coil in Figure 8. The αH resonances of residues from Phe4 to Arg13 can be seen to be largely upfield shifted, whereas those from Phe20 to Arg28 showed a smaller upfield shift. His14, Lys16, and Ser18, the residues linked to the three Pro residues, showed significant downfield shifts in the αH resonances. The conformational shifts from the NH resonances consistently showed slightly larger values than those from the αH resonances but these shifts were toward downfield as opposed to upfield shift of Hα resonances. These large chemical shift deviations from the random coiled values further support the presence of a helix covering residues 3−14 (segment I), and a bent conformation in the peptide range 15−20 (segment II). The small chemical shift deviations from the segment III (residues 20−28) may indicate a mixture of rapidly interconverting conformation.

Description of the 3D Structural Model. On the basis of the secondary structure analysis above, 11 3D structural models of the LP2 peptide have been built using Felix 95 and Insight II NMR program packages. Figure 9 shows overlay of 11 structures obtained with the constraints from the NOESY map, and an average structure is high-lined with a ribbon. The segments I and II of the peptide have ordered structures with 0.8 rmsd, and the segment III showed disordered conformation. The overall shape of the peptide can be described as a bend conformation in which the three prolines (residues 15, 17, and 19) are in the center of the bend. The NH_2-terminal part of the peptide folded into a stable helical conformation, and the C-terminal part of the peptide shows a mixture of rapidly interconverting conformations.

Insertion of the LP2 Peptide into Micelles. The micelles formed from DPC were used as membrane model providing a heterogeneous amphiphilic environment. Because of its small size (about 56 monomers in the absence of added protein), the micelles undergo isotropic motion, yielding a high-resolution spectrum for any peptide or protein that is incorporated in the interior, compared to use of large size micelle detergents (*30*). DPC (550 mM) was allowed to prepare monomeric peptide in a micelle, which has been used to generate a high-resolution NMR spectrum for synthetic membrane-bound peptides (*16*, *17*). Identical conditions were adopted for our LP2 peptide studies. The spin-labeled 12-doxylstearic acid was used to determine the membrane insertion residues of the LP2 peptide. The spin label produces selective broadening of 2D NMR resonances belonging to the residues buried in hydrocarbon region (*16*, *17*, *31*, *32*). The covalent attachment of the spin-labeled

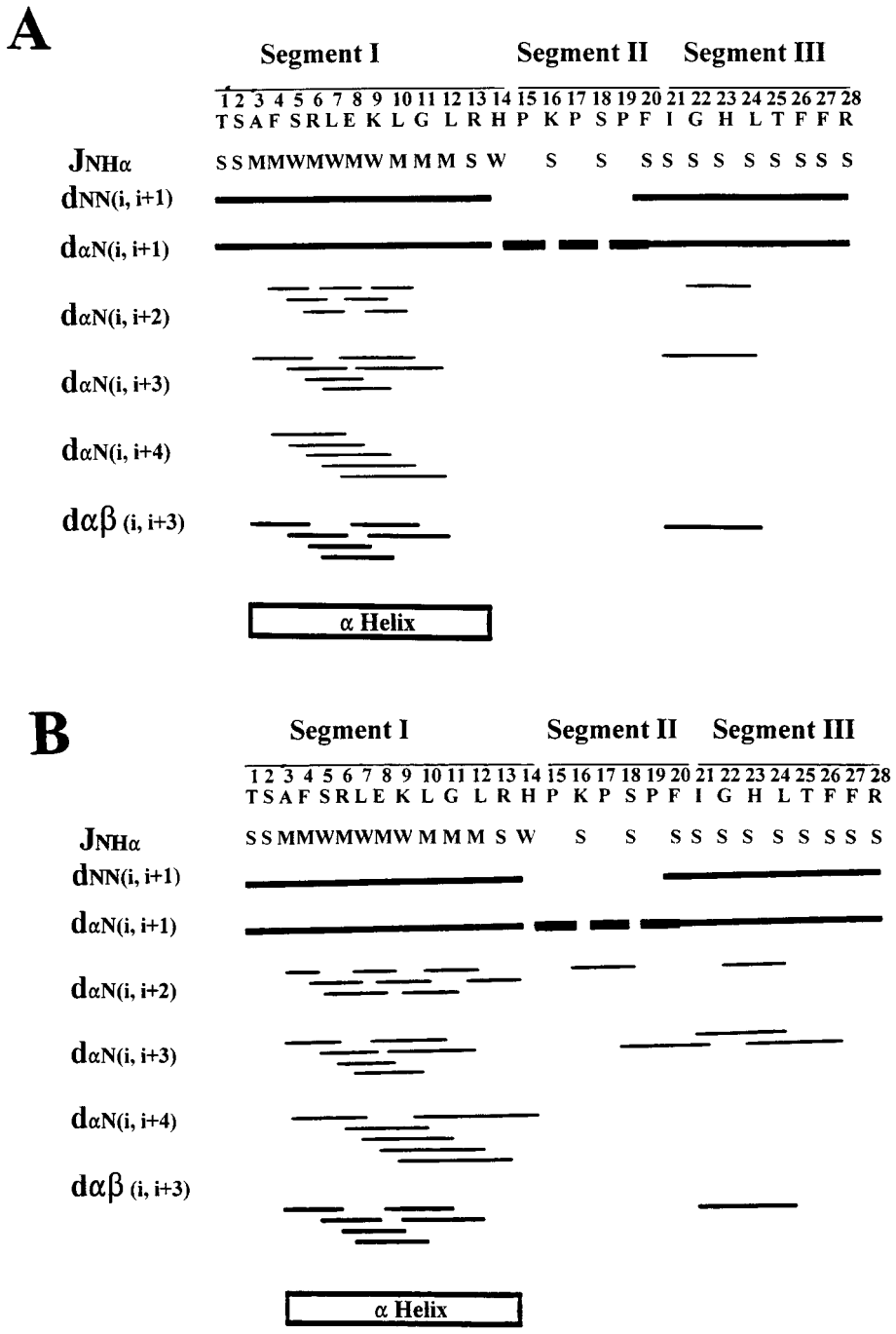

FIGURE 6: Amino acid sequence of TXAS LP2 and a survey of sequential and medium-range NOEs, spin-spin coupling constants of the peptide in TFE (A) and DPC micelles (B). The value of $^3J_{NH\alpha}$ coupling constant are reported in the notations of S (strong $J > 6$ Hz), M (medium $J = 4-6$ Hz), and W (weak $J < 4$ Hz), respectively. For the sequential NOE connectivities dαN and dNN (dNδ, and d$\alpha\delta$ for Xxx-Pro), thick and thin bars represent strong and weak NOE intensities. Medium-range NOEs dαN(i,i+1), dαN(i,i+2), dαN(i,i+3), dαN(i,i+4), and d$\alpha\beta$(i,i+3) are indicated by lines starting and ending at the position of the interacting residues. At the bottom of the figure, the location of helixes structure is shown.

Table 2: NOE Connectivities for Xxx(i)-Pro(i+1) Pairs in LP2[a]

Xxx-Pro	NH-CδH2	NH-CαH	CαH-CδH2	CαH-CαH
His14-Pro15	N	N	W	N
Lys16-Pro17	W	N	S	N
Ser18-Pro19	W	N	S	VW

[a] N = no NOE; W = weak NOE; VW = very weak NOE; S = strong NOE.

stearic acid at position 12 locates the free radical species in the center of the micelles (*16*, *17*). A comparison of the cross-peak intensities in the expanded region of LP2 peptide NOESY spectra in the absence and presence of 12-doxyl-stearic acid is shown in Figure 10. The cross-peak intensities of the residues located in the helical segment were dramatically suppressed (Figure 10B). The cross-peaks of the three proline residues (Pro15, 17, and 19) in the bent segment were also highly affected by the spin label. In segment III (residues 21−28), only the resonances of some hydrophobic residues (Phe20, 26, and 27) were affected by the spin label. This indicates that segment III is not immersed in the micelles and only makes discontinuous contact to the micelle.

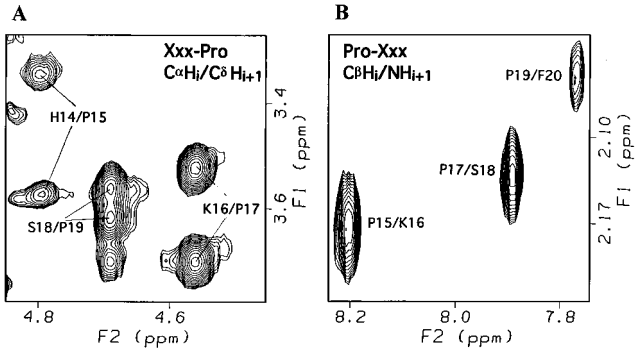

FIGURE 7: Interresidue cross peaks in the regions of CδHi/CβHi+1 (A, Xxx-Pro) and CβHi/NHi+1 (B, Pro-Xxx) of the 1H NOESY spectrum.

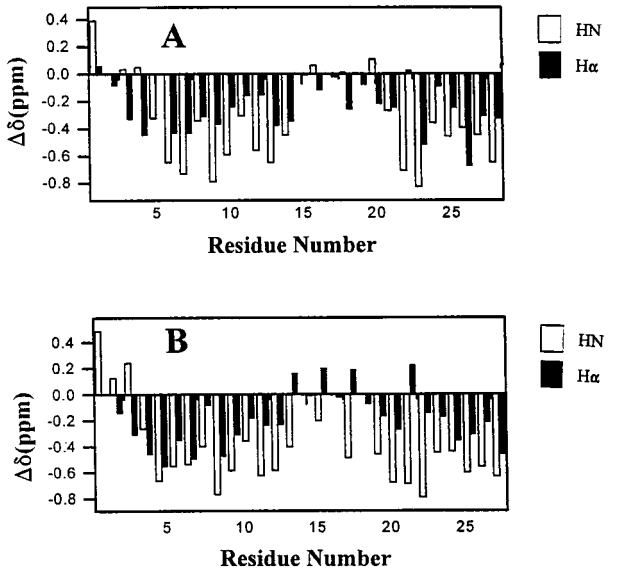

FIGURE 8: Plot of the differences between Hα and NH chemical shifts observed and the random coil chemical shifts described in text. (A) The peptide in TFE; (B) the peptide in DPC micelles.

Binding of Synthetic Peptides to Liposomes. In most cases, protein membrane anchor elements are thought to adopt a helix, whose hydrophobic side chains interact with the hydrocarbon interior of the phospholipid bilayer. Synthetic peptides corresponding to the LP2 segment I and to combined segments II and III were tested for binding to liposomes. As expected from the above results, the peptide corresponding to segment I (residues 33−46) was strongly associated with liposomes, whereas the peptide corresponding to segment II and III (residues 47−60) did not bind the liposomes (Figure 11). These results confirm that the this helical part of the second putative TXAS membrane anchor located within the segment I region is indeed capable to function as a membrane anchor.

DISCUSSION

No crystallographic structures are available yet for any membrane-bound P450 due to the difficulty of crystallization of membrane bound proteins. Several 3D structural models of the catalytic domains of mammalian P450s have been constructed using molecular modeling based on the crystal structures of the soluble bacterial P450s including P450cam (*33*, *34*), P450terp (*35*), and P450BM3 (*36*, *37*). However, the structure of the crucial NH_2-terminal membrane anchor segments of mammalian P450s could not be deduced because the available soluble P450 structures lack membrane anchor domains.

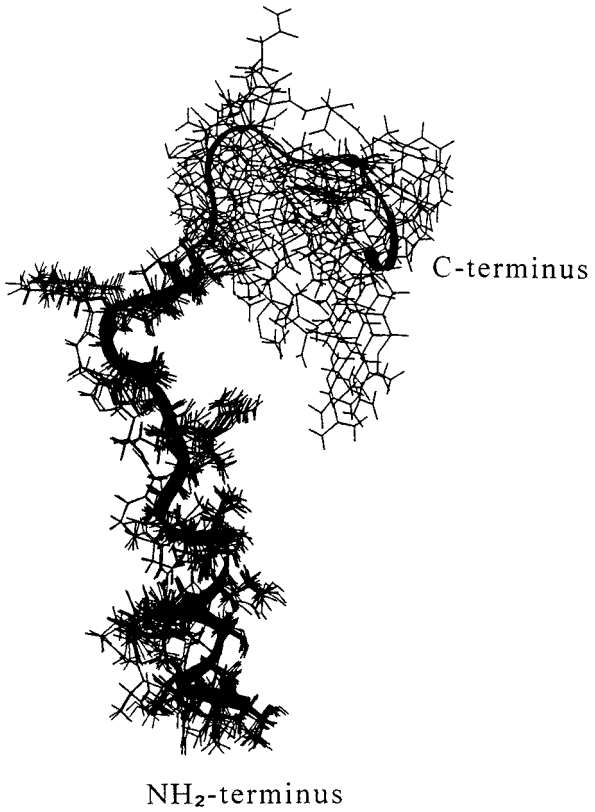

FIGURE 9: Overlay of eleven 3-D structural models of the LP2 peptide obtained by using the NMR refinement programs within Insight II package after dynamic studies and energy minimization. The structures of the side chains were added by using molecular modeling approach.

The aim of this work is to characterize the structure and the detailed topology of the second potential membrane anchor region of TXAS, which associated with liposomes. The CD data demonstrate that, upon addition of TFE or DPC to LP2, the interactions of the peptide with micelles induce α-helical formation from a random coil. The 2D NMR data confirmed the α-helical structure of the peptide in micelles and help to define the α-helical segment in the N-terminal portion of the peptide. The membrane topology and anchor function of the helical segment have been further elucidated by determining the specific spin relaxation effect of the spin-labeled lipid and liposome incorporation studies.

Normally about 18 residues of a conventional helical structure are needed to cross a lipid bilayer in a single membrane-spanning domain (*38*, *39*). The N-terminal α-helical segment of TXAS LP2 peptide accounts only 14 residues. Thus, it was expected that part of segment II (peptide residues 15−20) would also be immersed in the membrane. This exception was supported by the spin-labeled 2D NMR results, which revealed that the cross-peaks of the three proline residues totally disappeared upon the addition of the hydrophobic spin-labeled probe (Figure 10). These results agree with the previous studies, in which proline residue(s) were observed in putative membrane insertion regions of membrane-bound proteins (*40*).

For the segment III of TXAS LP2, the intensities of cross-peaks of the hydrophobic residues, such as in the spin-labeled

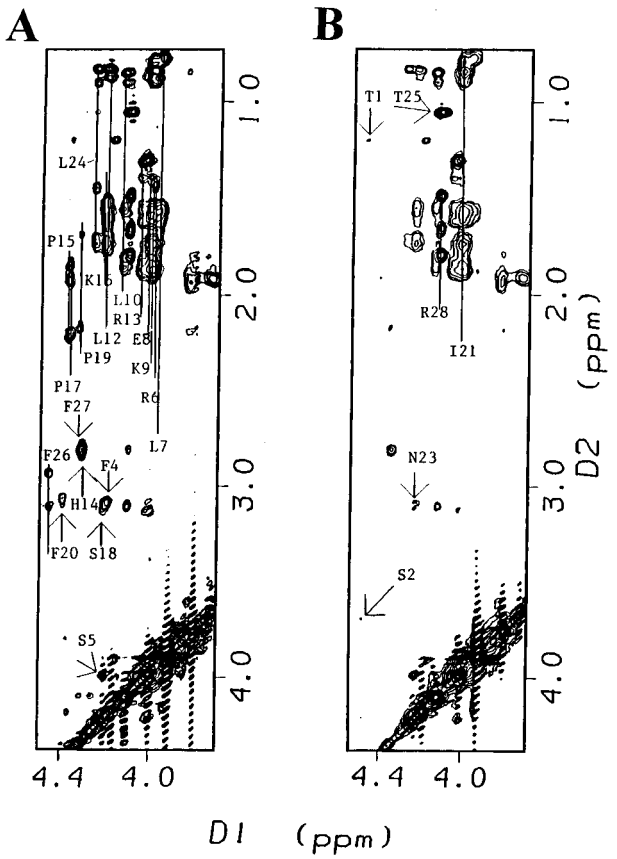

FIGURE 10: Comparison of expanded region of NOESY spectra of TXAS LP2 peptide in DPC micelles in the absence (A) and presence (B) of 12-doxylstearic acid. Resonances which were not affected by the presence of 12-doxylstearic acid are shown in panel B.

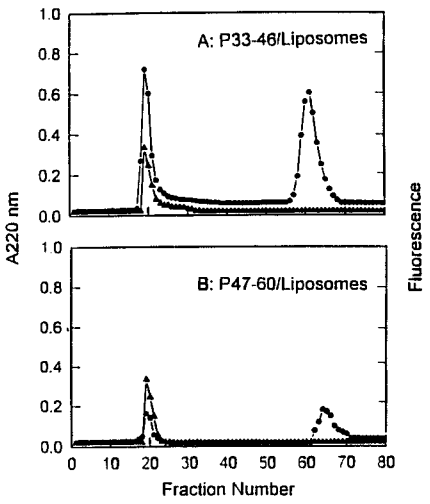

FIGURE 11: Incorporation of peptide TXAS P33−46 (LP2 residues 1−14) and P47−60 (LP2 residues 15−28) to lipid vesicles. Gel filtration chromatography of Sepharose 6B was used to analyze liposome mixtures prepared with P33−46 (A) and P47−60 (B). Individual fractions (1.0 mL) were monitored spectrophotometrically at 220 nm (circles) and fluorometrically at 420 nm after addition of diphenylhexatriene (triangles). Details are described in the Materials and Methods.

NMR were reduced, while the hydrophilic residues were not affected. It suggested that the segment III has an amphipathic structure with a buried location for the hydrophobic side and an exposure location for the hydrophilic side in micelles. The orientation of segment III appears on the surface of the membrane with insertion of the hydrophobic side into the membrane. This feature agrees with the bent conformation in segment II of the peptide. Taken together all these data allow us to propose an initial membrane anchor model for the second potential membrane anchor region of TXAS bound to ER membrane with following features: (1) the peptide segment I (TXAS residues 33−46) with an α-helical structure belongs to the main part of the membrane anchor region; (2) the peptide segment II (TXAS residues 47−52) including the three proline residues, with a bent conformation, is an extension of the segment I bound to the membrane and toward the membrane surface; (3) due to the bent structure of segment II, peptide segment III (TXAS residues 53−60) extends along the surface of the membrane and contacts the membrane with only its hydrophobic residues to form an amphipathic structure.

In comparison with the sequences of P450 family 3 which have the highest sequence identities with TXAS, the helical segment I of TXAS LP2 only shares 28% sequence identity (*1*) which is much less than other regions. However, the proline-rich segment II and the adjacent segment III of the TXAS LP2 peptide are highly conserved in other microsomal P450s (>50% sequence identity) (*1*). These suggest that other P450s may not necessarily have similar secondary structures and membrane anchor functions in the helical segment. It also suggests that the functional residues for the membrane anchor may be only located in the helical segment I of the LP2 peptide. The peptidoliposome reconstitution studies with two other synthetic peptides, corresponding to segment I or II-III, supported the suggestion (Figure 11). Only the helical segment I of the LP2 peptide functionally binds to liposomes, and the peptide covering the segments II and III does not have a binding function to the liposomes. The partial insertion of segment II in the membrane and surface contacts of segment III with the membrane of the LP2 peptide are due to the segment I anchor in the membrane.

It should be noted that TXAS shares considerable primary and secondary structure with other cytochrome P450s (*4*, *5*). However, the NH_2-terminal six residues of TXAS appear to make up an additional "tail" segment that extends beyond the NH_2-terminus of other microsomal P450s (*1*). This unique NH_2-terminal structure makes it unclear what degree of the membrane anchor structure of TXAS resembles that of other membrane-bound p450s composition. To this end, the existence of multiple membrane anchor segments has been demonstrated in several microsomal P450s, which remain membrane-associated even after deletion of 29−30 residues of the hydrophobic first segment of the NH_2-terminal domain (*41*, *42*). Characterization of the second putative membrane anchor region of TXAS provides a clue for testing the membrane anchor region(s) for other P450s and suggests a possibility of different membrane anchor format presence in TXAS.

ACKNOWLEDGMENT

We thank Drs. Richard J. Kulmacz and Kenneth K. Wu for valuable discussions while this study was in progress and Dr. Hong Davis for technique assistance. The acknowledgment is also made to the Robert A. Wetch Foundation (E-1270) and the W. M. Keck Center for Computational Biology for computer resource support.

REFERENCES

1. Ruan, K.-H., Wang, L.-H., Wu, K. K., and Kulmacz, R. J. (1993) *J. Biol. Chem. 268*, 19483−19489.
2. Ruan, K.-H., Li, P., Kulmacz, J. R., and Wu, K. K. (1994) *J. Biol. Chem. 269*, 20938−20942.
3. Wang, L.-H., Ohashi, K., and Wu, K. K. (1991) *Biochem. Biophys. Res. Commun. 177*, 286−299.
4. Yokoyama, C., Miyata, A., Ihara, H., Uilrich, V., and Tanabe, T. (1991) *Biochem. Biophys. Res. Commun. 178*, 1479−1484.
5. Ohashi, K., Ruan, K., Kulmacz, R. J., Wu, K. K., and Wang, L.-H. (1992) *J. Biol. Chem. 267*, 789−793.
6. Shen, R.-F, Back, S. J., Zhang, L., Chase, M. B., Tai, H.-H., and Purtell, D. C. (1992) *Eighth Int. Conf. on prostaglandins and related compounds*.
7. Haurand, M., and Ullrich, V. (1985) *J. Biol. Chem. 260*, 15059−15067.
8. Black, S. D. (1992) *FASEB J. 6*, 680−685.
9. Merrifield, R. B. (1963) *J. Am. Chem. Sci. 85*, 2149−2154.
10. Merrifield, R. B., Vizili, L. D., and Boman, H. G. (1982) *Biochemistry 22*, 1970−1974.
11. Ruan, K. H., Stiles, B. G., and Atassi, M. Z. (1991) *Biochem. J. 274*, 849−854.
12. Moore, W. T., and Caprioli, R. M. (1991) in *Techniques in Protein Chemistry II* (Villafranca, J. J., Ed.) pp 511−528, Academic Press, New York.
13. Zvi, A., Hiller, R., and Anglister, J. (1992) *Biochemistry 31*, 6972−6979.
14. Chen, Y. H., Yang, T. J., and Chau, K. H. (1974) *Biochemistry 13*, 3350−3359.
15. Whthrich, K. (1986) *NMR of Proteins and Nucleic Acids*, John Wiley & Sons, New York.
16. Chupin, V., Killian, J. A., Breg, J., de Jongh, H. H. J., Boelens, R., Kaptein, R., and de Kruijff, B. (1995) *Biochemistry 34*, 11617−11624.
17. Chupin, V., Leenhouts, J. M., de Kroon, A. I. P. M., and de Kruijff, B. (1996) *Biochemistry 35*, 3141−3146.
18. Whthrich, K., Billeter, M., and Braun, W. J. (1983) *J. Mol. Biol. 169*, 949−961.
19. Kunz, B. C., Rehorek, M., Hauser, H., Winterhalter, K. H. and Richter, C. (1985) *Biochemistry 24*, 2889−2895.
20. Englander, S. W., and Wand, A. J. (1987) *Biochemistry, 26*, 5953−5958.
21. Chazin, W. J., Rance, M., and Wright, P. E. (1988) *J. Mol. Biol. 202*, 603−622.
22. Basus, V. J. (1989) *Methods Enzymol. 177*, 132−149.
23. Braunschweiler, L., and Ernst, R. R. (1983) *J. Magn. Reson. 53*, 521−528.
24. Bax, A., and Davis, D. G. (1985) *J. Magn. Reson. 61*, 306−320.
25. Rance M., Srrensen, O. W.,Bodenhausen, G., Wagner, G., Ernst, R. R., and Whthrich, K. (1983) *Biochem. Biophys. Res. Commun. 117*, 479−485.
26. Jeener, J., Meier, B. H., Bachmann, P., and Ernst, R. R. (1979) *J. Chem. Phys. 71*, 4546−4553.
27. Wishart, D. S., Sykes, B. D., and Richards, F. M. (1992) *Biochemistry 31*, 1647−1651.
28. Bystrov, V. F. (1976) *Prog. Nucl. Magn. Reson. Spectros. 10*, 41−82.
29. Pardi, A., Billeter, M., Braun, W., and W. thrich, K. (1984) *J. Mol. Biol. 180*, 741−751.
30. Henry, G. D., and Sykes, B. D. (1992) *Methods Enzymol. 239*, 515−534.
31. Brown, L. R., Braun, W., Kumar, A., and Whthrich, K. (1982) *Biophys. J. 37*, 319−328.
32. Papavoine, C. H. M., Konings, R. N. H., Hilbers, C. W., and Van De Ven, F. J. M. (1994) *Biochemistry 33*, 12990−12997.
33. Johnson, E. F., Kronbach, T., and Hsu, M.-H. (1992) *FASEB J. 6*, 700−705.
34. Zvelebil, M. J., Wolf, C. R., and Sternberg, M. J. E. (1991) *Protein Eng. 4*, 271−282.
35. Hasemann, C. A., Ravichandran, K. G., Petersonn, J. A., and Deisenhofer, J. (1994) *J. Mol. Biol. 236*, 1169−1185.
36. Tarr, G. E., Black, S. D., Fujita, V. S., and Coon, M. J. (1983) *Proc. Natl. Acad. Sci. U.S.A. 80*, 6552−6556.
37. Ruan, K.-H., Milfeld, K., Kulmacz, R. J., and Wu, K. K. (1994b) *Protein Eng. 7*, 1345−1351.
38. Masibay, A. S., Balaji, P. V., Boeggeman, E. E., and Qasba, P. K. (1993) *J. Biol. Chem. 268*, 9908−9916.
39. Bretscher, M. S., and Munro, S.(1993) *Science 261*, 1280−1281.
40. Polinsky, A., Goodman, M., Williams, K. A., and Deber, C. M. (1992) *Biopolymers 32*, 399−406.
41. Larson, J. R., Coon, M. J., and Porter, T. D. (1991) *J. Biol. Chem. 266*, 7321−7324.
42. Yabusaki, Y., Murakami, H., Sakaki, T., Shibata, M., and Ohkawa, H. (1988) *DNA 7*, 701−711.

BI971881Y